ORIGINAL ARTICLE

NF-κB regulates brown adipocyte function through suppression of ANT2

Shiqiao Peng[a], Xiaoying Zhang[a], Lili Yu[b], Yanhong Xu[c], Yang Zhou[d], Shengnan Qian[a], Xinyu Cao[a], Xiaotong Ye[d], Jiajun Yang[c], Weiping Jia[a], Jianping Ye[a,e,f,*]

[a]*Shanghai Diabetes Institute, Shanghai Jiao Tong University Affiliated Sixth People's Hospital, Shanghai 200233, China*
[b]*Department of Immunology, School of Basic Medical Sciences, Xinxiang Medical University, Xinxiang 453003, China*
[c]*Neurology Department, Shanghai Jiao Tong University Affiliated Sixth People's Hospital, Shanghai 200233, China*
[d]*National Demonstration Center for Experimental Fisheries Science Education, College of Fisheries and Life Science, Shanghai Ocean University, Shanghai 201306, China*
[e]*Metabolic Disease Research Center, Zhengzhou University Affiliated Zhengzhou Central Hospital, Zhengzhou 450007, China*
[f]*Center for Advanced Medicine, College of Medicine, Zhengzhou University, Zhengzhou 450007, China*

Abstract The transcription factor nuclear factor of kappa-light-chain-enhancer of activated B cells (NF-κB) is expressed in brown adipocytes, but its role remains largely unknown in the cells. This issue was addressed in current study by examining NF-κB in brown adipocytes *in vitro* and *in vivo*. NF-κB activity was increased by differentiation of brown adipocytes through elevation of p65 (RelA) expression. The transcriptional activity of NF-κB was induced by the cold stimulation with an elevation in S276 phosphorylation of p65 protein. Inactivation of NF-κB in brown adipocytes made the knockout mice [uncoupling protein 1 (*Ucp1*)−CreER−p65[f/f], U-p65-KO] intolerant to the cold environment. The brown adipocytes exhibited an increase in apoptosis, a decrease in cristae density and uncoupling activity in the interscapular brown adipose tissue (iBAT) of p65-KO mice. The alterations became severer after cold exposure of the KO mice. The brown adipocytes of mice with NF-κB activation (p65 overexpression, p65-OE) exhibited a set of opposite alterations with a reduction in apoptosis, an increase in cristae density and uncoupling activity. In mechanism, NF-κB inhibited expression of the adenine nucleotide translocase 2 (ANT2) in the control of apoptosis. Data suggest that NF-κB activity is increased in brown adipocytes

by differentiation and cold stimulation to protect the cells from apoptosis through down-regulation of ANT2 expression.

1. Introduction

Brown adipocytes and beige (brite) adipocytes are thermogenic adipocytes, which play a central role in non-shivering thermogenesis in the prevention of hypothermia upon cold exposure of mammals. This group of adipocytes contributes to maintenance of energy balance by releasing excess energy as heat. The biological significance of brown adipose tissue (BAT) and beige fat extends far beyond the energy expenditure into regulation of glucose/lipid metabolism, insulin sensitivity and adipose tissue homeostasis through the endocrine activity[1,2]. Regulation of the thermogenic function represents a strategy in the management of obesity and diabetes. There have been a dozen of potential molecular targets documented in the management of differentiation and function of the thermogenic adipocytes[3]. However, a druggable target remains missing in the strategy[1]. Apoptosis inhibits the thermogenic function of brown/beige cells[4]. Anti-apoptosis is an ideal strategy in the induction of brown/beige cell function. Unfortunately, apoptosis-related molecules remain largely unknown in the control of brown/beige cell functions except p53[4]. The transcription factor nuclear factor of kappa-light-chain-enhancer of activated B cells (NF-κB) has a well-known anti-apoptotic activity in addition to the inflammatory activity. However, the anti-apoptosis activity remains to be established in brown adipocytes. This issue is addressed in current study.

It is generally believed that pro-inflammatory signals inhibit the function of brown/beige adipocytes as reported for some representative cytokines including tumor necrosis factor alpha (TNF-α), interleukin 1 beta (IL-1β), transforming growth factor-β (TGF-β), etc.[1] However, there are exceptions as the pro-inflammatory cytokine IL-6 promotes differentiation and thermogenic function of beige adipocytes[5,6]. In addition, the anti-inflammatory cytokine IL-10 inhibits the thermogenic function of BAT[7,8]. A couple of signaling pathways, such as inhibitor of kappa B kinase beta (IKKβ)/NF-κB, c-Jun N-terminal kinase (JNK)/activated protein 1 (AP1), Janus kinase (JAK)/signal transducers and activators of transcription (STAT), etc., are activated by these cytokines. The exact role of each pathway remains to be established in the brown/beige adipocytes. NF-κB activation is induced by IKKβ in the inflammatory responses. The transcriptional activity of NF-κB is determined primarily by the p65 (RelA) subunit through heterodimerization with the p50 subunit in most type of cells. Inactivation of NF-κB promotes apoptotic response in white adipocytes as reported in the studies of fat-selective p65-knockout (KO) and Ikkβ-KO mice[9,10]. Induction of NF-κB activity by overexpression of p65 (p65-OE) or IKKβ (IKKβ-OE) in adipocytes enhances energy expenditure in the transgenic mice leading to the resistance to diet-induced obesity[9,11]. Alternatively, activation of NF-κB activity by deletion of p50 (that negatively regulates p65 transcriptional activity) also promotes energy expenditure[9]. These studies suggest that NF-κB may be required for the thermogenic function of brown/beige adipocytes. However, the possibility remains to be tested.

In this study, we examined NF-κB activity in brown adipocytes and identified conditions for its activation by non-inflammation signals. The functional significance of NF-κB was tested in interscapular brown adipose tissue (iBAT) depot of the KO mice [uncoupling protein 1 (Ucp1)-CreER-p65$^{f/f}$, U-p65-KO] and p65-OE mice. NF-κB activity was found to protect the brown adipocytes through down-regulation of adenine nucleotide translocase 2 (ANT2) in the control of apoptosis.

2. Materials and methods

2.1. Animals

All mice were on the C57BL/6 genetic background. Two lines of transgenic mice were used in this study. The first is brown adipocyte-selective p65 KO mice, which were established by crossing p65-floxed mice[12] with tamoxifen inducible Ucp1−CreER mice, a gift from Professor Christian Wolfrum at ETH Zurich, Schwerzenbach, Switzerland. Genotype of the mice is Ucp1−CreER−p65$^{f/f}$ (U-p65-KO). The littermate p65$^{f/f}$ (p65-floxed) mice were used in the control. The second line of mice was adipocyte P2 (aP2)−p65 mice, in which p65 gene overexpression is controlled by the fatty acid binding protein 4 (Fabp4) gene promoter[9]. All mice were produced in-house at the animal facility of the Shanghai Jiao Tong University Affiliated Sixth People's Hospital [specific pathogen free (SPF) grade; Shanghai, China]. The facility environment is 12-h light cycle with ambient temperature of 22 ± 2 °C. The animals were used at 8 weeks in age and fasted for 10 h before the experiment. All procedures and operations in the mouse experiments were approved by the Institutional Animal Care and Use Committee (IACUC) in the Shanghai Jiao Tong University Affiliated Sixth People's Hospital (Shanghai, China).

2.2. Body temperature and thermal imaging

Ucp1−p65-KO mice were fed on Chow diet and the study was conducted at 8 weeks in age. The mice were treated with tamoxifen by gavage at 100 mg/kg/day for 5 days to induce Cre expression. On Day 7, the mice were individually housed and exposed to 4 °C ambient temperature for 2 or 7 h. The body temperature was measured in the mice by a rectal thermometer (Type C Thermometer, Therma Waterproof, American Fork, UT, USA). The body temperatures were recorded at different time points in the cold response study. Thermal imaging camera (SMART SENSOR ST9450 Infrared Thermal Imaging Camera IR Thermography, Everett, WA, USA) was used to detect the interscapular surface temperature of the mice.

2.3. Cristae density and mitochondrial superstructure

iBAT depots were collected from the anesthetized mice and fixed in the electron microscope fixing solution (Servicebio technology,

Wuhan, China) immediately. The tissue volume was about 1 mm^3, and fixation was for 2 h at room temperature and 4 h at 4 °C. The tissue was embedded with 1% agarose and washed in 0.1 mol/L phosphate buffer (pH 7.4) for 3 times at 15 min each time. The tissue was treated in 1% osmium, 0.1 mol/L phosphate buffer at room temperature for 2 h and wash for 3 times. Tissues were successively dehydrated in 50%, 70%, 80%, 90%, 95%, and 100% alcohol, 100% acetone for 15 min each time and were permeated through acetone: 812 embedding agent in a 1:1 ratio for 4 h, in a 1:2 ratio overnight, and 812 embedding agent for 8 h in the end. The embed tissues were kept at 60 °C for 48 h. Ultramicrotome (Leica, Wetzlar, Germany) was used to slice the tissues at 60−80 μm in thickness. Stain the sections with 2% uranium acetate saturated ethanol solution and lead citrate for 15 min separately. After the sections were dried overnight at the room temperature, the structure of tissues was observed and analyzed in a Philips CM12 transmission electron microscope (Philips/FEI, Eindhoven, Netherlands). Mitochondria diameter and cristae density were analyzed using ImageJ Software (version 1.50b, National Institutes of Health, Bethesda, MD, USA). The mitochondrion shape was defined by the axis ratio of the oval that fits the organelle area best. Mitochondrial number was counted, the longest diameter was measured in each mitochondrion and the mean value was obtained from three images of a sample at 30,000 times of magnification. Cristae were identified manually in the electron microscope images and cristae density was defined by the ratio of the total points hitting cristae over the total points hitting the mitochondria. Each data point represents the mean value of three images per sample in three mice of each group.

2.4.   Hematoxylin and eosin (H&E) staining

The fresh iBAT tissues were fixed in 4% paraformaldehyde for 24 h before the H&E staining. The samples were prepared by the Wuhan Servicebio technology Co., Ltd. (Wuhan, China).

2.5.   Mitochondrion isolation

iBAT was quickly collected from the anesthetized mice and put into MSE [including 210 mmol/L mannitol, 70 mmol/L sucrose, 1 mmol/L EGTA, and 0.5% bovine serum albumin (BSA), pH 7.2] on ice. The tissues were washed twice with MSE and cut into small pieces with the surgical scissors followed by homogenization. All operations were carried out on ice. The supernatant was collected after centrifugation at 4 °C, 600 ×g for 10 min into a new tube. The pellet was collected after centrifugation at 7000 ×g for 10 min as isolated mitochondria. The mitochondria were purified with washing in MSE and centrifuged at 4 °C, 7000 ×g for 10 min twice. The purified mitochondria were resuspended in MAS (including 220 mmol/L mannitol, 70 mmol/L sucrose, 5 mmol/L MgCl$_2$·6H$_2$O, 10 mmol/L KH$_2$PO$_4$, 2 mmol/L HEPES, 1 mmol/L EGTA, and 0.2% BSA, pH 7.2) and kept on ice for functional assays.

2.6.   Oxygen consumption rate (OCR) of isolated mitochondria

The probe plate of 24-well was pretreated with the hydration solution (1 mL per well) at least 12 h in advance in a CO$_2$-free incubator at 37 °C. The substrates in the assay were prepared in MAS. Mitochondrial protein concentration was measured with the bicinchoninic acid (BCA; Beyotime, Nanjing, China) method, and the loading volume of tested sample was calculated according to

the protein concentration. The inhibitor bongkrekic acid (BA; Santa Cruz BioTechnology, CA, USA) or agonist carboxyatractyloside (Carb; Absin, Shanghai, China) were injected into four injection holes from A to D according to the experimental protocol. The chemicals were 4 mmol/L adenosine diphosphate (ADP; Sigma−Aldrich, St. Louis, MO, USA), 2 μmol/L oligomycin (Sigma−Aldrich), 4 μmol/L carbonyl cyanide 4-(trifluoromethoxy) phenylhydrazone (FCCP; Selleck Chemicals, Houston, TX, USA), and 4 μmol/L antimycin (Santa Cruz BioTechnology). The mitochondria were loaded into the plate at 5 μg/100 μL per well according to the protein concentration. The plate was centrifuged at 2200 ×g 4 °C for 20 min to let mitochondria to precipitate, and 350 μL MAS was added into each well with substrates followed by analysis with Seahorse Analyzer XFe24 (Agilent Technologies, Santa Clara, CA, USA).

2.7.   Primary brown adipocytes

The primary brown adipocytes were obtained by differentiation of ear mesenchymal stem cells of mouse in vitro. The mice were sacrificed by cervical dislocation after anesthesia, the ears were quickly collected and cleaned by removing hair, washing in 75% ethanol and phosphate buffered saline (PBS) containing 1% penicillin−streptomycin for 3 times, respectively. The ears were cut into small pieces and digested with type 1 collagenase in a water bath at 37 °C for 2 h. The ear mesenchymal stem cells were collected in pellet after centrifugation at 157 ×g for 5 min. The cells were resuspended in Dulbecco's modified Eagles medium (DMEM; Gibco, Life Technologies Corporation, USA) medium [containing 10% fetal bovine serum (FBS) and 1% penicillin−streptomycin (Gibco)] and placed into a 10 cm plate and cultured in a CO$_2$ (5%) incubator of 37 °C. The DMEM medium was changed every 3 days. At 70%−80% confluence, the cells were divided into 2 plates for passage. At 100% confluence, the cells were treated with differentiation-inducing cocktails for 6−8 days in differentiation into the primary brown adipocytes, in which the cocktail I (5 nmol/L insulin, 0.5 mmol/L IBMX, 2 nmol/L T$_3$, 1 μmol/L dexamethasone, and 5 μmol/L rosiglitazone; Sigma−Aldrich) was used for 4 days and the cocktail II (5 nmol/L insulin and 2 nmol/L T$_3$; Sigma−Aldrich) was used for 2−4 days. The differentiation medium was changed every 2 days. Differentiation was carried out in a 10% CO$_2$ incubator (Panasonic Corporation, Osaka, Japan). After differentiation, the cells were maintained in the normal medium in a 5% CO$_2$ incubator and the medium was changed at 24 h before the experiment.

2.8.   Quantative reverse transcription PCR (qRT-PCR)

mRNA was quantified with qRT-PCR according to a protocol reported elsewhere[13]. The RNA Extraction Reagent (R401-01, Vazyme Biotech, Nanjing, China) was used to extract total RNA from brown adipocytes or tissue, and the concentration was determined with SpectraMax i3× (Molecular Devices, San Jose, CA, USA). mRNA was then transcribed into cDNA using the HiScript® II Q RT SuperMix (R223-01, Vazyme Biotech) and quantified with ChamQ™ Universal SYBR qPCR Maser Mix (Q711-02, Vazyme Biotech) on Light Cycle 480II (Roche, Pleasanton, CA, USA). The primers were synthesized as follow: Il-6: forward, 5′-CTCCCAACAGACCTGTCTATAC-3′; reverse, 5′-CCATTGCACAACTCTTTTCTCA-3′; 18S: forward, 5′-GCCGCTAGAGGTGAAATTCT-3′; reverse, 5′-TCGG

AACTACGACGGTATCT-3′. All results were normalized to the 18S mRNA level.

2.9. Respiration of brown adipocytes

The primary ear mesenchymal stem cells were plated into XFe24 plate at 3×10^4 cells/well and differentiated into brown adipocytes after confluence as described above. The cells were cultured in the normal medium for at least 24 h before OCR assay. The probe plates were hydrated in a CO_2 free incubator one day in advance. The brown adipocytes were washed in the test solution (25 mmol/L dextrose monohydrate, 1 mmol/L sodium pyruvate, and 4 mmol/L glutamine in base medium, pH 7.4) twice, at 500 μL each time, and then 500 μL of test solution was added in each well and incubated in CO_2 free incubator at 37 °C for 1 h. For adenoviral transient infection, the ANT2 adenoviruses [multiple of infection (MOI), 1:100] were added into the adipocytes (3×10^6 cells per well) for 48 h without obvious cytopathic effects to knockdown or overexpress ANT2. The modification efficiency was determined by Western blot assay. During incubation, the probe plate was injected with oligomycin (1 μmol/L), FCCP (2 μmol/L), rotenone (0.5 μmol/L), and antimycin (0.5 μmol/L), and then examined with the Seahorse Analyzer. The Wave 2.6.1.53 software (Agilent Technologies) was used to analyze the data and calculate ATP production, proton leakage, etc.

2.10. Western blot

The expression of interest proteins was quantified by Western blot according to the protocol described[14]. The primary antibodies included in this manuscript were listed in Supporting Information Table S1. The signal was detected with chemiluminescent detection system (E412-01-AA, Western Lightning ECL; Vazyme Biotech), the images were collected with a CCD camera system (Light-Capture; ATTO, Tokyo, Japan) and the signal was quantified with the ImageJ program for the statistical analysis.

2.11. Immunoprecipitation (IP)

IP assay was conducted by using a protocol described by previous study[15]. In brief, 500 μg of total protein were incubated with 2 μg antibodies (antibodies included: BCL-xL, BCL-2, and Bax; Abcam, Cambridge, UK) and 20 μL of 50% protein G agarose (Beyotime), mixed, and constantly rotated overnight at 4 °C. After incubation was performed, the supernatant was aspirated, and the beads were saved. The beads were washed six times using cold 0.1% NP-40 lysis buffer and boiled for 5 min at 100 °C in 2× sodium dodecyl sulfate polyacrylamide gel electrophoresis (SDS-PAGE) loading buffer. The complexes in supernatant were loaded onto SDS-PAGE gel for Western blot analysis.

2.12. Statistical analysis

All data were quantified for statistical analysis. The body temperature data were statistically analyzed with two-way ANOVA. In vitro experiments were repeated at least three times with consistent results and the digital data were statistically analyzed with the Student's t-test. The data are presented as mean ± standard deviation (SD) with $P < 0.05$.

3. Results

3.1. NF-κB activation in brown adipocytes

NF-κB activity was examined in the primary brown adipocytes in two conditions to characterize its activation, in vitro cell differentiation and in vivo cold stimulation. In the first condition, NF-κB activity was gradually increased by differentiation of the primary mesenchymal cells, which was observed with elevated protein level of P65, the major subunit of NF-κB. The maximal level was reached on Days 5 and 6 of differentiation (Fig. 1A). mRNA was increased in the same pattern as the protein (Fig. 1B). P50 protein and mRNA were not changed by the differentiation (Fig. 1A and B). The patterns of P65 and P50 changes in brown adipocyte differentiation are similar to those of white adipocytes in differentiation[16]. In the second condition, NF-κB activity was tested in iBAT after exposure of mice to the cold environment, in which phosphorylation status of P65 at S276, an activation marker, was significantly induced by the cold stimulation (Fig. 1C). As expected, UCP-1 protein was increased in iBAT under the same condition (Fig. 1C). Il-6 (a target gene of NF-κB) expression was increased in iBAT under the same condition (Fig. 1D). A role of β3-adrenergic receptor in the NF-κB activation was investigated in vitro. The phosphorylation was induced by the β3-adrenergic receptor agonist, CL-316243 (10 μmol/L), together with IL-6 expression in the primary brown adipocytes (Fig. 1E and F). The observations suggest that NF-κB activity is increased in brown adipocytes by differentiation and cold stimulation to regulate gene expression.

3.2. Dysfunction of iBAT in U-p65-KO mice

It was reported that NF-κB activity is required by white adipocytes for cell survive, adipose tissue remodeling and expansion in the study of p65-KO mice[12], Ikkβ-KO mice[10] and Iκbα mice[17]. However, the NF-κB activity remains to be established in brown adipocytes. To address the issue, NF-κB was inactivated in brown adipocytes in the U-p65-KO mice by crossing the p65-floxed mice with Ucp1−CreER mice. The U-p65-KO mice exhibited cold intolerance with a significant drop in the core body temperature during cold exposure (Fig. 2A). The skin temperature over iBAT was monitored with a thermosensitive camera to determine the BAT function. A significant reduction was observed in the U-p65-KO mice (Fig. 2B and C). Apoptosis in iBAT was examined to explore the mechanism of the cold intolerance. A significant increase in apoptosis was observed with the elevated level of cleaved caspase 3 in U-p65-KO mice after the cold exposure (Fig. 2D). In the wild type (WT) mice, the apoptotic signal was not increased in iBAT under the same condition (Fig. 2E). A significant reduction in p65 and IκBα protein were observed in iBAT of U-p65-KO mice to confirm the gene inactivation (Fig. 2F). Those data suggest that inhibition of NF-κB activity by p65 gene
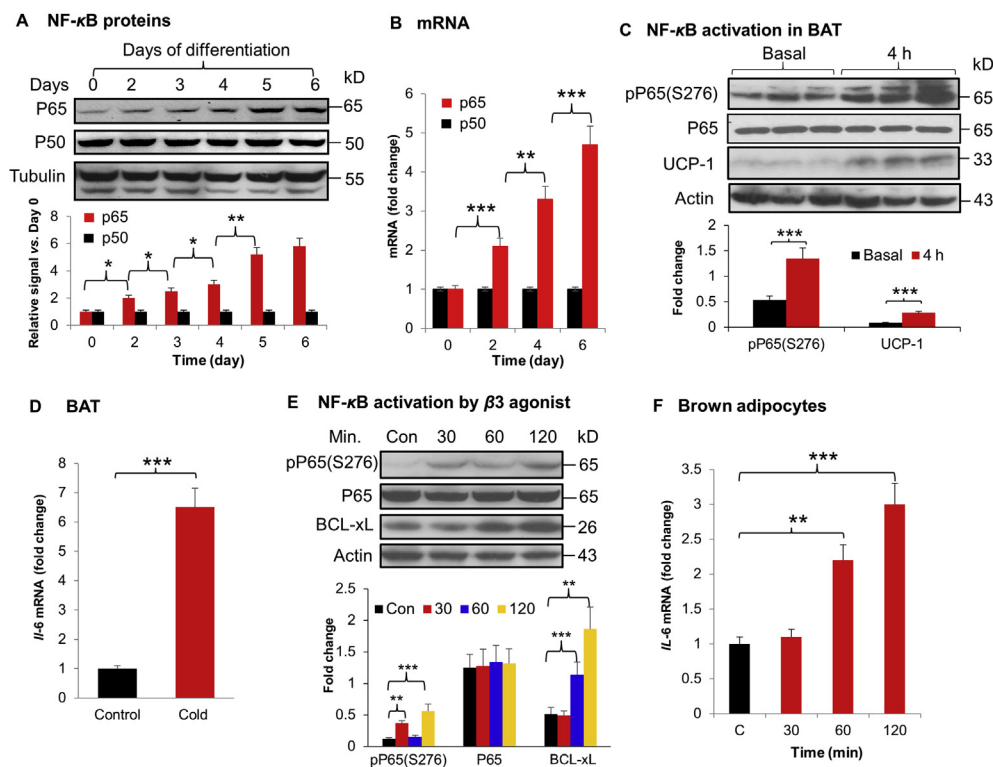
Figure 1 NF-κB activation in brown adipocytes. The primary mesenchymal cells were differentiated for 4 days in the cocktail containing 0.5 mmol/L IBMX, 125 μmol/L indomethacin, 1 μmol/L dexamethasone, 20 nmol/L insulin, and 1 nmol/L T3, and followed by additional 4 days of differentiation in medium containing 20 nmol/L insulin and 1 nmol/L T3. (A) Proteins of P65 and P50. The whole cell lysate was used in Western blot (WB) with antibodies to P65 and P50. WB signals were quantified and expressed in relative signal strength over that of Day 1. (B) mRNA levels of p65 and p50. mRNA level was determined by qRT-PCR on days of differentiation indicated. (C) NF-κB activation in BAT of WT mice after 4 h of cold challenge ($n = 6$). (D) *Il-6* mRNA in BAT of WT mice after 4 h cold stimulation ($n = 6$). (E) NF-κB activation by β3 agonist. The primary brown adipocytes of WT mice were examined for NF-κB activation after a β3-adrenergic receptor agonist (CL-316243, 10 μmol/L) treatment at different times (30, 60, and 120 min) as indicated by WB. (F) *Il-6* mRNA expression. mRNA level was determined by qRT-PCR. The cell culture studies were repeated three times in this study with consistent results. Representative blots are shown. Each bar represents mean ± SD ($n = 6$). *$P < 0.05$, **$P < 0.01$, ***$P < 0.001$.

inactivation may impair the thermogenic function of iBAT through induction of apoptosis, which was supported by the impaired cold response and elevated apoptosis in iBAT of U-p65-KO mice.

3.3. Reduced cristae density in mitochondria by p65-KO

The apoptosis was investigated in brown adipocytes by analysis of ultrastructure of mitochondria. Mitochondrial cristae is formed by the inner membrane and the cristae density is a structural indicator of mitochondrial function. The density was examined under the transmission electron microscope. A significant reduction was found in the brown adipocytes of U-p65-KO mice without the cold exposure. Cristae was broken in the mitochondrial matrix for the density fall in the KO mice (Fig. 3A). In addition, mitochondrial swelling was observed in the KO adipocytes for the shape change, further suggesting the structural damage. The structural defects became more severe in U-p65-KO mice after 4 h response to the cold (Fig. 3B). The cold response induced membrane rupture in mitochondria for matrix leaking into the cytosol in the KO mice. The observations were supported by quantification of the ultrastructure image (Fig. 3C and D). The cell density was examined in iBAT and an increase was observed in U-p65-KO with lower

triglyceride content in the brown adipocytes in H&E staining (Fig. 3E and F). The differences in iBAT were observed between KO and WT mice before the cold exposure, and they became dramatic after the cold exposure. These data suggest that p65 deficiency leads to impairment in the mitochondrial ultrastructure and a reduction in the lipid droplets in the cytoplasm of brown adipocytes.

3.4. ANT2 up-regulation by p65-KO

In search for the mechanism of mitochondrial damage, we screened the genes in iBAT of U-p65-KO mice by RNA sequencing, which led us to focus on ANT2 (AAC2) for its increased expression in the KO mice (Supporting Information Table S2). ANT2 belongs to the ANT family, a nucleus-encoded mitochondrial protein that contains 4 members (ANT1, ANT2, ANT3, and ANT4) for proton transportation in thermogenesis[18]. An increase in the activity leads to cell apoptosis through collapse of mitochondrial potential[19]. However, the ANT2 activity remains unknown in iBAT of p65-KO mice. ANT1 and ANT2, the ubiquitously expressed isoforms, were investigated in the WT mice in response to the cold challenge, and a reduction in both isoforms was observed in iBAT (Fig. 4A). In the U-p65-KO mice, the two
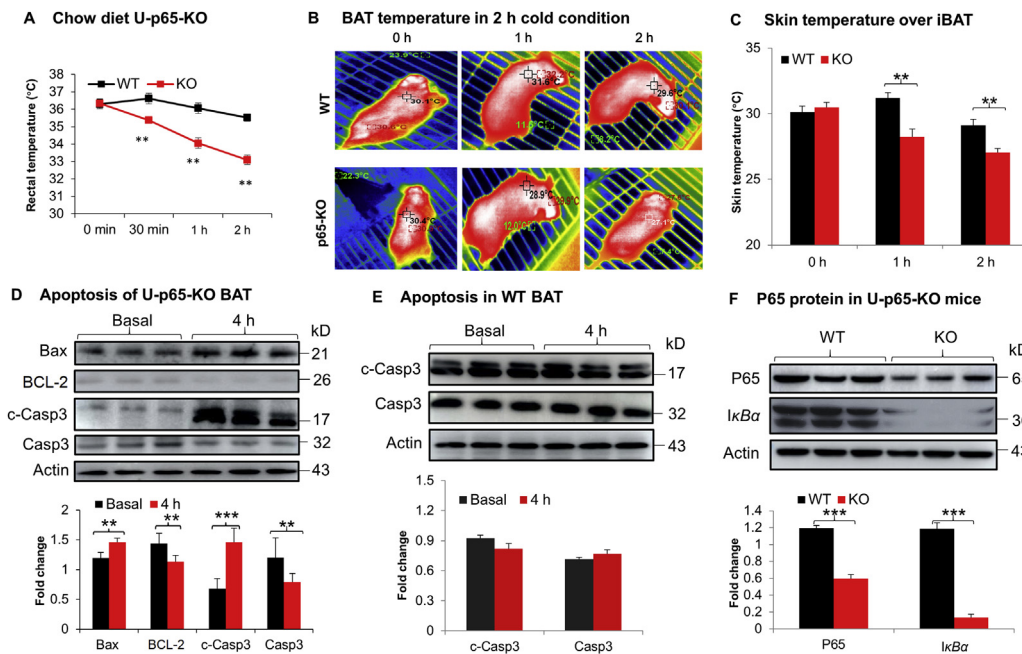
Figure 2   Impaired BAT function in U-p65-KO mice. (A) Body temperature of U-p65-KO mice in the cold response. UCP1-p65-KO (U-p65-KO) and the control mice (p65-floxed) were fed on Chow diet, which were used at 8 weeks in age. The mice were injected with tamoxifen at 100 mg/kg/day for 5 days to induce Cre expression for the p65 knockout. At seven days post the last injection, the mice were individually housed at 4 °C ambient temperature for 2 h and the core body temperature was monitored with an annal thermometer (n = 6). *P < 0.01 vs. WT group. (B) Infrared imaging of skin temperature over iBAT. The images were taken from the mice under 4 °C ambient temperature with a thermal imaging camera for the skin temperature over iBAT. (C) Mean value of the skin temperature recorded in the study of panel B (n = 6). (D) Apoptosis in iBAT of U-p65-KO mice. The apoptosis signals were detected in iBAT by WB after 4 h cold stimulation of UCP1-p65-KO mice (n = 3). (E) Apoptosis in iBAT of WT mice (n = 3). (F) Confirmation of P65 protein reduction in BAT of U-p65-KO mice. Representative images are shown in this figure (n = 3). In the bar figure, each bar represents mean ± SD (n = 3). **P < 0.01, ***P < 0.001. Casp3, caspase 3; c-Casp3, cleaved caspase 3.

isoforms exhibited different patterns of changes, in which ANT2 protein was elevated and ANT1 was not altered (Fig. 4B). UCP-1 protein was not altered in iBAT of U-p65-KO mice. The ANT2 elevation was associated with a significant increase in apoptosis for the cleaved caspase 3 and reduced B cell lymphoma/lewkmia-2 (BCL-2) (Fig. 4C). An interaction of ANT2 with the BCL family proteins was investigated in immunoprecipitation to understand the ANT activity in apoptosis. The interactions with anti-apoptotic proteins, such as BCL-2 and BCL-xL, were significantly reduced in the KO mice (Fig. 4D), suggesting that reduced interaction of ANT2 and anti-apoptotic proteins may contribute to the increased apoptosis in the U-p65-KO cells. To test the possibility, ANT2 protein was reduced in the p65-KO cells by shRNA-mediated knockdown to match the level of WT cells (Fig. 4E), which led to a reduction in the c-caspase 3 signal to block the apoptotic phenotype of the p65-KO cells (Fig. 4F). The data suggest that in the physiological condition, ANT1 and ANT2 were reduced in WT brown adipocytes to protect the cells from apoptosis upon the cold stimulation. The response was interrupted in U-p65-KO cells by the elevated ANT2 leading to the higher risk of apoptosis for the impaired iBAT function.

3.5.   ANT2 in mitochondrial uncoupling activity

The impact of ANT2 in mitochondrial respiration was examined by monitoring the respiration parameter OCR, whose alteration reflects the coupling (ATP production) and uncoupling activities

(thermogenesis). The respiration was tested in two models, the isolated mitochondria of iBAT and primary brown adipocytes. ANT2 activities were induced with the chemical agonist Carb, and suppressed with the chemical inhibitor BA. The ANT activation by Carb promoted the uncoupling activity in isolated mitochondria of the WT mice, which was observed with an elevated OCR following the FCCP treatment (Fig. 5A). The uncoupling was unaffected by the inhibitor BA (Fig. 5A). In the KO mice, the same responses were observed in the isolated mitochondria. The data suggest that ANT2 activation may raise the uncoupling activity in the WT and KO brown adipocytes. ANT2 elevation in the KO cells may enhance the uncoupling activity of mitochondria. However, the result was opposite to the prediction. The uncoupling activity was decreased in the mitochondria of U-p65-KO mice for a reduction in the maximal OCR (Fig. 5B). ANT2 activation by Carb could not fix the defect in U-p65-KO cells (Fig. 5A). The essential role of ANT2 was tested by Ant2 knockdown (KD). The uncoupling activity was significantly reduced by the knockdown in the WT cells (Fig. 5C), but not in the KO cells (Fig. 5D). The basal oxygen consumption was inhibited more in the KO cells by ANT2-KD relative to the WT cells (Fig. 5D). Mitochondrial potential was increased by the knockdown in WT cells (Fig. 5E), which was likely a result of inhibition of proton leak and ATP production. The same effect was observed in the KO cells (Fig. 5F). The data suggest that ANT2 is required for the uncoupling activity of brown adipocytes in the physiological condition in WT cells.
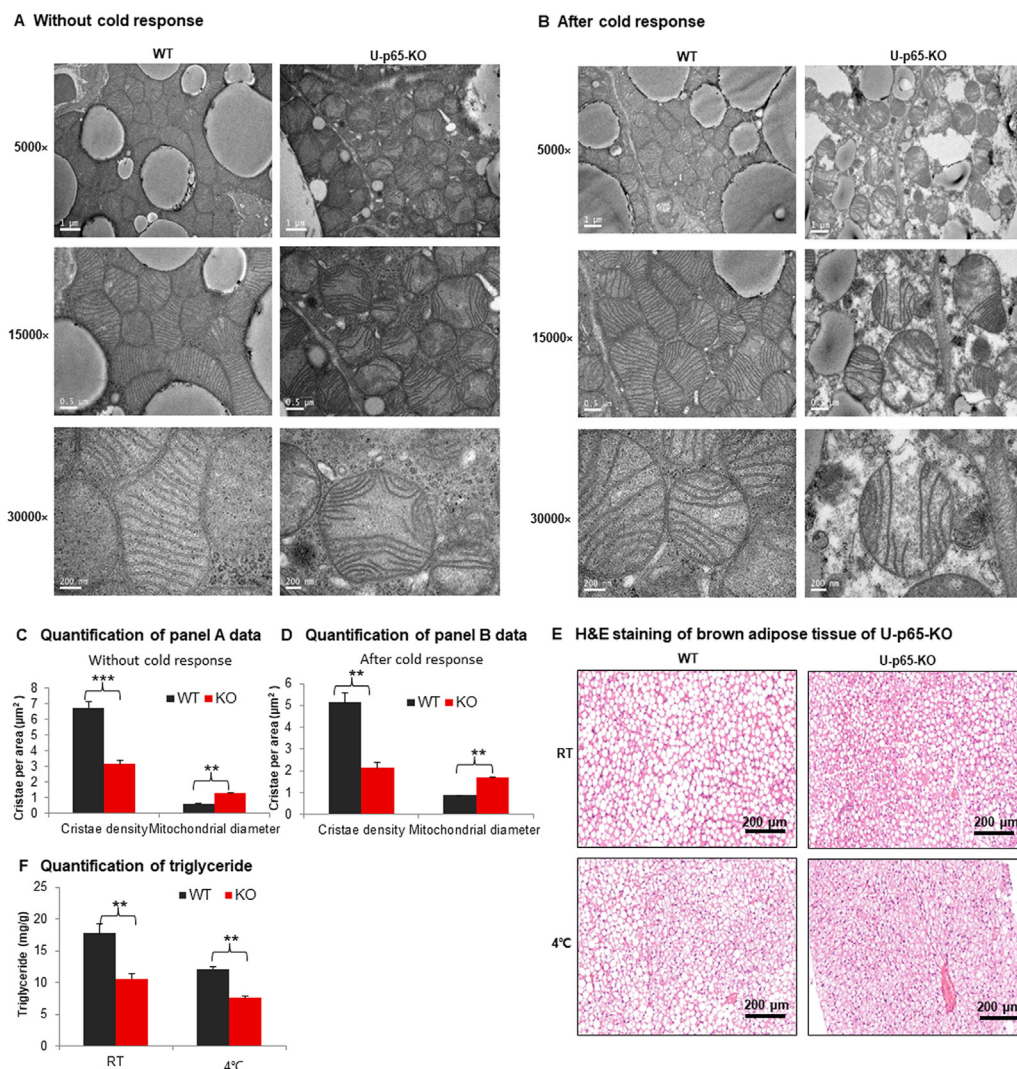
Figure 3 Mitochondrial super structure in the brown adipocytes of U-p65-KO mice. (A) Mitochondria in the brown adipose tissue of U-p65-KO mice without the cold exposure. The brown adipose tissues were collected and fixed in the electron microscope fixing solution immediately and used in the superstructure analysis with transmission electronic microscope. (B) Mitochondria in the brown adipose tissue of U-p65-KO mice after 4 h of the cold exposure. Scale bar: 1 μm (5000×), 0.5 μm (15,000×), and 200 nm (30,000×), respectively. (C) and (D) Quantification of panels A and B images. (E) H&E staining of brown adipose tissue of U-p65-KO. The study was conducted in mice with and without the cold exposure. Scale bar: 200 μm. (F) Triglyceride quantification in BAT. In the bar figure, each bar represents mean ± SD ($n = 6$). **$P < 0.01$, ***$P < 0.001$. RT, room temperature.

The elevated ANT2 did not promote, instead reduced the uncoupling activity in the p65-KO cells, which could not be restored by ANT2-KD. The data suggest that ANT2 elevation may not play a major role in the thermogenic defects in iBAT of U-p65-KO mice.

3.6. ANT2 down-regulation by p65-OE

Above results suggest that ANT2 may be down-regulated by NF-κB in brown adipocytes as its level was increased in p65-KO cells. To test the possibility, the ANT2 activity was investigated in p65-OE mice (p65 mice). A significant reduction was observed in ANT2 protein and no alteration was observed in ANT1 protein in the same condition (Fig. 6A). The increase in NF-κB activity was confirmed in iBAT of the p65 mice with elevated P65 and IκBα proteins (Fig. 6A). UCP-1 protein was not altered by the NF-κB

activity (Fig. 6A). Consistently, apoptosis was significantly reduced in iBAT of p65 mice by the reduced levels of cleaved caspase 3, Bax, and elevated BCL-xL (Fig. 6B). No significant change was observed in BCL-2 protein. In the ANT2/BCL family interaction, Bax was reduced, BCL-2 and BCL-xL were not changed in iBAT of p65 mice (Fig. 6C). The data suggest that ANT2 protein was decreased by NF-κB to prevent apoptosis in the brown adipocytes. To test the possibility, the ANT2 level was restored in the primary brown adipocytes of p65 mice with an ANT2 expression adenovirus (Fig. 6D and E). Interestingly, the resistance to apoptosis was cancelled by the ANT2 restoration (Fig. 6F). The impact of NF-κB in mitochondrial ultrastructure was examined, the cristae density was increased and mitochondrial size was reduced in the p65 mice (Fig. 6G−J). The data suggest that NF-κB decreases ANT2 protein in the mechanism of anti-apoptosis phenotype of iBAT of p65 mice.
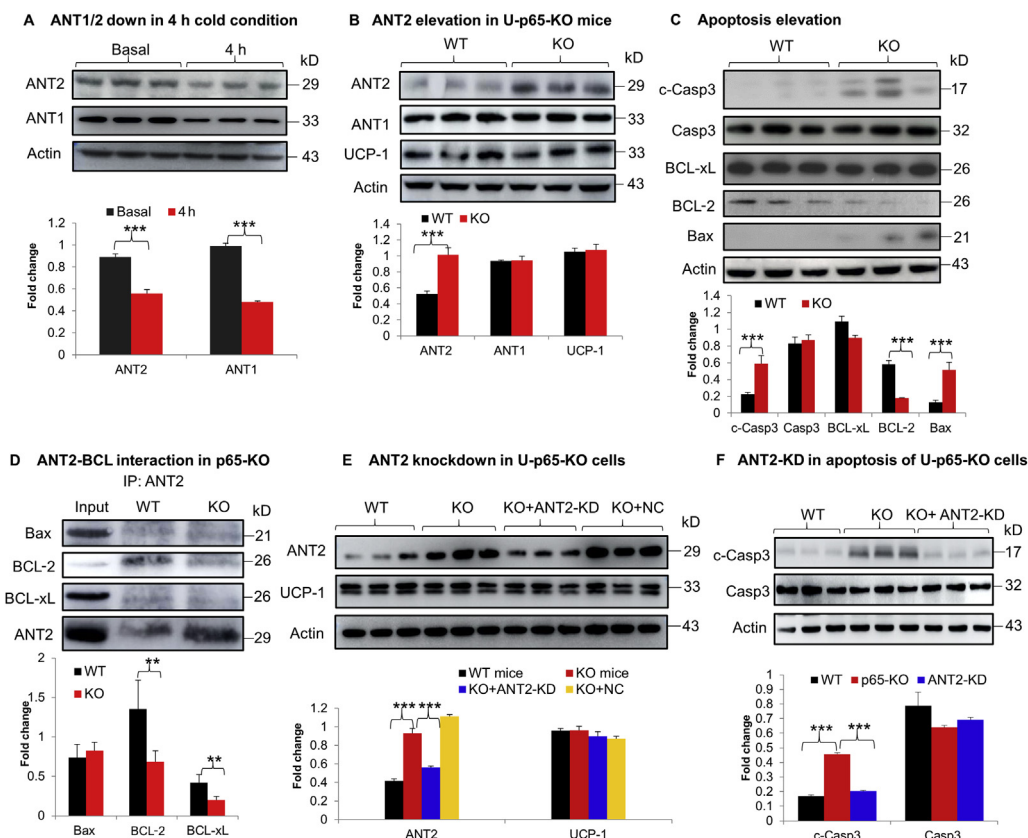
Figure 4 ANT2 was increased in BAT tissue of U-p65-KO mice. (A) ANT2 reduction in iBAT of WT mice by cold exposure. (B) ANT2 elevation in BAT of U-p65-KO mice. The study was conducted at 8 weeks in age without cold challenge. (C) Apoptosis in U-p65-KO mice ($n = 3$). (D) Interaction of ANT2 and BCL family proteins in the brown adipose tissue of U-p65-KO mice. The study was conducted by immunoprecipitation of ANT2 and blotted with antibodies to the BCL proteins including Bax, BCL-2, and BCL-xL. The immune complex was resolved by 12% SDS-PAGE. Each experiment was repeated three times in this study. (E) ANT2 knockdown in U-p65-KO mice. *Ant2* was knocked down in the primary brown adipocytes of U-p65-KO mice with shRNA to *Ant2* (ANT2-KD) delivered by adenovirus. The virus of scrambled shRNA was used as the negative control (NC). (F) Apoptosis after Ant2-KD. Apoptosis was tested in the primary brown adipocytes after *Ant2* knockdown. Each experiment was repeated three times with consistent results in this study. Representative blots were shown. In the bar figure, each bar represents mean ± SD ($n = 3$). *$P < 0.05$, **$P < 0.01$, ***$P < 0.001$.

3.7. Enhanced uncoupling in p65-OE cells

The impact of ANT2 reduction in mitochondrial function was investigated in the brown adipocytes of p65 mice. The uncoupling activity was examined in the isolated mitochondria in the group of p65 mice and the activity was significantly increased (Fig. 7A). The uncoupling activity was further enhanced by the ANT agonist (Carb) in the mitochondria (Fig. 7B). The effect of ANT2 reduction was further investigated with ANT2 restoration by gene overexpression in the brown adipocytes of p65 mice. ANT2 overexpression enhanced the uncoupling activity in the groups of WT cells (Fig. 7C). In the p65 mice, the restoration by overexpression promoted the uncoupling activity (Fig. 7D). The impact of ANT2 reduction in mitochondrial potential was further investigated. A reduction was observed in the brown adipocytes of p65 mice, which was reduced further by ANT2 overexpression (Fig. 7E). ANT2 overexpression in WT cells also decreased the potential (Fig. 7F), which is likely a result of more proton leak through ANT2. In the cold environment, the thermogenic function of iBAT was increased in p65 mice as indicated by the skin temperature over iBAT (Fig. 7G). The data suggest that the decreased ANT2 activity may not be responsible for the increased

uncoupling activity and reduced mitochondrial potential in p65 mice. The mechanism remains unknown for the functional phenotype of brown adipocytes in the p65 mice.

4. Discussion

Current study demonstrated that NF-κB activity was increased in the brown adipocytes by differentiation from preadipocytes and by the cold stimulation. The p65 expression was increased in the differentiated brown adipocytes, and its phosphorylation was enhanced by the cold stimulation. The data suggest that NF-κB has multiple activities in the brown adipocytes, such as control of apoptosis and thermogenesis. The anti-apoptotic activity was established in iBAT of U-p65-KO mice by the increased signal of cleaved caspase 3. The mice became intolerant to the cold with a quick reduction in the body temperature. The increased apoptosis was associated with decreased thermogenesis in the U-p65-KO mice under cold stimulation. In the p65-OE mice, the apoptosis was reduced and thermogenic function was enhanced. The decreased apoptosis was coupled with the rise in thermogenesis in p65-OE mice. The data suggest that NF-κB activity is required for iBAT function. This NF-κB activity has never been characterized
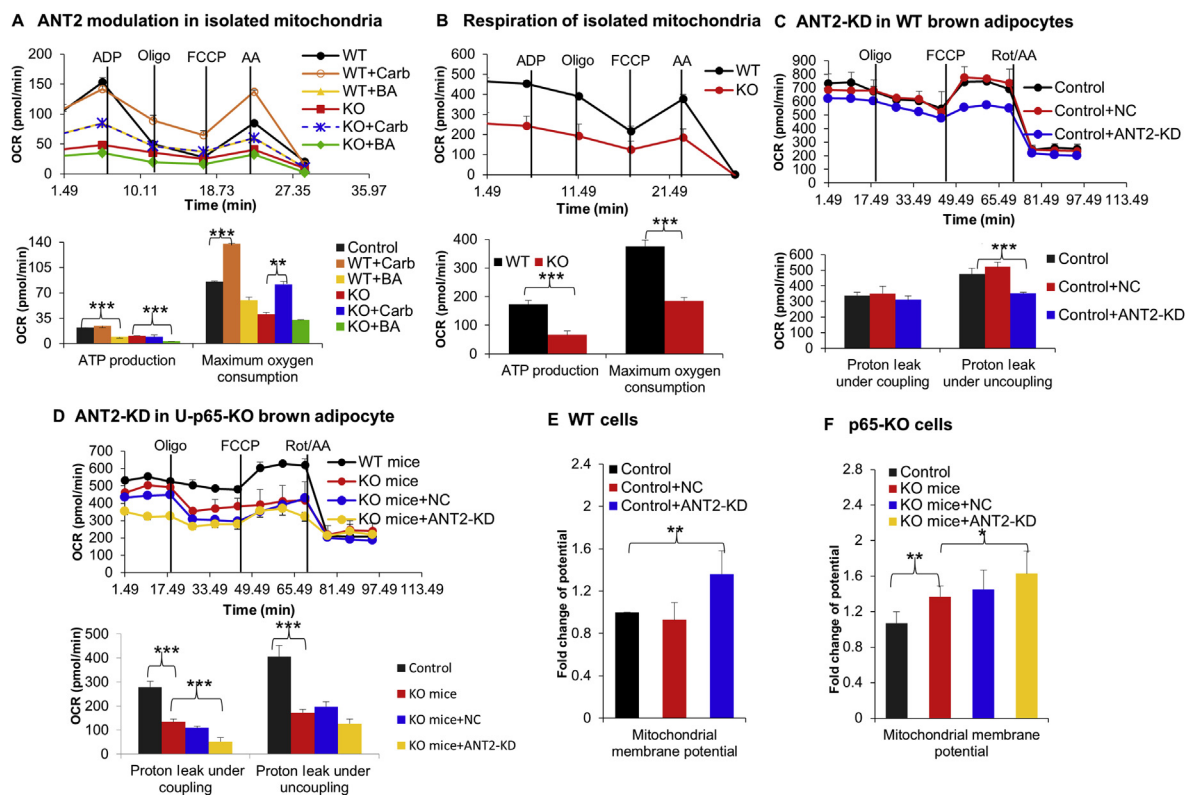
Figure 5 ANT2 elevation restricted uncoupling activity in U-p65-KO cells. (A) ANT2 impact in the uncoupling function. Mitochondria were isolated from fresh BAT and were tested for uncoupling function in MAS with 10 mmol/L succinate and 2 μmol/L rotenone (Rot). OCR was monitored in mitochondria (10 μg) in response to the chemicals and calculated for the uncoupling activity. The chemicals were ADP (4 mmol/L), oligomycin (2 μmol/L), FCCP (4 μmol/L), antimycin A (AA, 4 μmol/L). The isolated mitochondria were tested in the mitochondria assay solution (MAS) containing 10 mmol/L succinate and 2 μmol/L rotenone treated with ANT2 agonist carboxyatractyloside (Carb, 20 μmol/L) and inhibitor bongkrekic acid (BA, 5 μmol/L), respectively ($n = 3$). (B) Respiration in isolated mitochondria. Mitochondria (10 μg/well) were isolated from BAT and the uncoupling activity was investigated by analyzing the oxygen consumption rate (OCR) alteration using the Seahorse equipment with the respiration complex activator or inhibitors including ADP (4 mmol/L), oligomycin (2 μmol/L), FCCP (4 μmol/L), antimycin A (4 μmol/L). ATP production and maximal OCR were calculated to compare the difference between WT and U-p65-KO ($n = 3-4$). (C) ANT2 knockdown did not affect the uncoupling of U-p65-KO brown adipocytes. The assay was conducted in the primary adipocytes ($n = 3$). The chemical concentrations were 1 μmol/L oligomycin, 2 μmol/L FCCP, 0.5 μmol/L rotenone plus 0.5 μmol/L antimycin A (Rot/AA). (D) ANT2 knockdown decreased the uncoupling function of WT brown adipocytes. Knockdown was conducted in the primary brown adipocytes (3×10^6 cells per well) and OCR was examined after 48 h of adenovirus infection. Proton leak under the coupling and uncoupling conditions were calculated with OCR. (E) Mitochondrial membrane potential. ANT2 was knocked down in the primary brown adipocytes with the isoform-specific shRNA (ANT2-KD) delivered by adenovirus, and the virus of scrambled shRNA was used in the negative control (NC). The potential was quantified in the cells with the fluorescent dye JC-1 by flow cytometry ($n = 3$). (F) Mitochondrial membrane potential after ANT2 knockdown in U-p65-KO brown adipocytes. The potential was quantified in the U-p65-KO brown adipocytes with the fluorescent dye JC-1 by flow cytometry. Each experiment was repeated three times in this study with consistent results. Representative blots were shown. In the bar figure, each bar represents mean ± SD ($n = 3$). $*P < 0.05$, $**P < 0.01$, $***P < 0.001$.

in brown adipocytes in other studies of iBAT according to the literature search at the PubMed database.

We observed that ANT2 was up-regulated to promote apoptosis in the brown adipocytes when NF-κB was inactivated by p65 gene deletion in U-p65-KO mice. ANT is a nucleus-encoded mitochondrial protein located in the inner membrane with a classical activity in the import of ADP and export of ATP. ANT2 is one of the 4 isoforms (ANT1, ANT2, ANT3, and ANT4)[20]. ANT was found to promote apoptosis a decade ago[21], but the action mechanism remained unclear till 2019 when the proton transporter activity was identified in ANT1[18], in which ANT1 (AAC1) was reported to mediate the proton leak in several types of tissues including heart and skeletal

muscle, etc. However, the role of ANT1 isoform, ANT2, remains to be established in apoptosis. Current study provides a series of evidence to support the ANT2 activity in apoptosis. Additionally, we identified NF-κB as a regulator of ANT2 activity. The data from U-p65-KO cells suggests that NF-κB increased mRNA expression of ANT2 to render brown adipocytes to apoptosis. The conclusion was approved by the reduced ANT2 expression and decreased apoptosis in the p65-OE cells. Although the conclusion was derived from the brown adipocytes, it may apply to other types of cells given the nature of ubiquitous expression of ANT2. *Ant2* gene knockdown has been reported in a couple of studies for insulin sensitization in mice[22,23]. However, mechanism of the knockdown
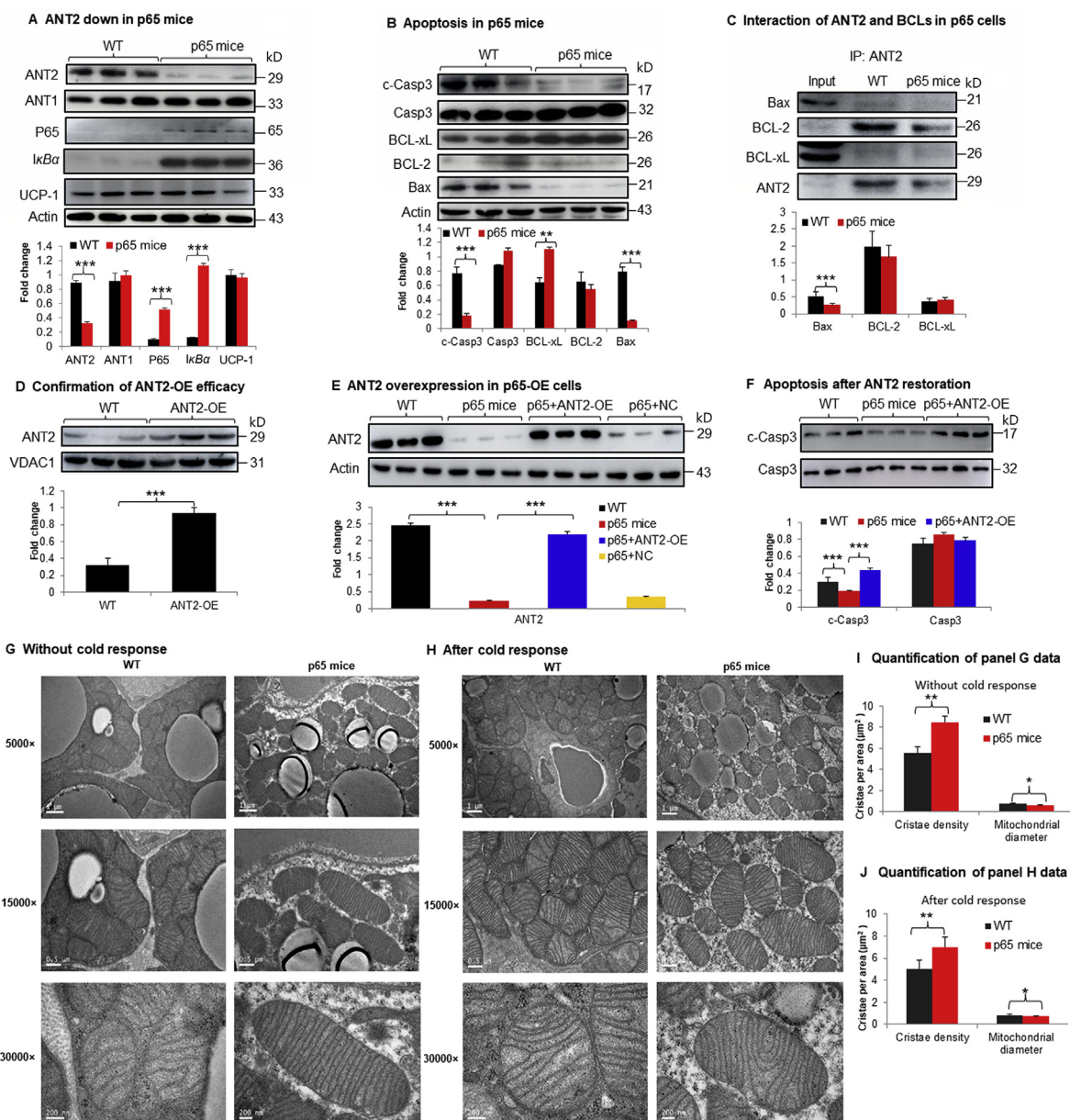
Figure 6 ANT2 was decreased in BAT tissue of p65-OE mice. (A) ANT2 in p65-OE mice. ANT2 protein was examined in BAT of p65-OE mice after 4 h cold exposure (*n* = 3). (B) Apoptotic proteins in p65 mice (*n* = 3). BCL family proteins were examined for apoptosis in BAT of p65 mice (*n* = 3). (C) Interaction of ANT2 and BCL proteins in immunoprecipitation. The assay was conducted in BAT of p65-OE mice and the immune complex of ANT2 antibody was blotted with antibodies to BCL-2, Bax, and BCL-xL. Whole cell lysate of BAT was used in the input as a control. (D) *Ant2* overexpression effect. Overexpression of *Ant2* was done in the primary brown adipocytes of WT mice. (E) Restoration of *Ant2* in p65-OE cells. (F) Apoptosis in p65-OE cells after *Ant2* restoration. The primary brown adipocytes were derived from stromal cells of p65 mice and infected with the ANT2 expression adenovirus. Apoptosis was examined in the cells by Western blot after ANT2 overexpression. (G) Electron microscope image of mitochondria before the cold challenge. (H) Electron microscope image of mitochondria after the cold challenge. Scale bar: 1 μm (5000×), 0.5 μm (15,000×), and 200 nm (30,000×), respectively. (I) Cristae density and mitochondrial size before the cold challenge. (J) Cristae density and mitochondrial size after the cold challenge. Each experiment was repeated three times in this study with consistent results. Representative blots are shown. In the bar figure, each bar represents mean ± SD (*n* = 3). *$P < 0.05$, **$P < 0.01$, ***$P < 0.001$.

benefit remains to be investigated. Current study suggests that the knockdown effects may be related to an increased resistance to cell apoptosis in the metabolic tissues. The mRNA change provided a mechanism for ANT2 regulation by NF-κB, but the exact event for *Ant2* mRNA alteration remains to be explored.

This study suggests that ANT2 is required for the uncoupling activity of mitochondria in the brown adipocytes. ANT1 (AAC1) was reported to involve in the thermogenic function of mitochondria in several types of cells including brown adipocytes[18]. In current study, the same activity of ANT2 was identified in brown adipocytes. Overexpression of ANT2 promoted the uncoupling
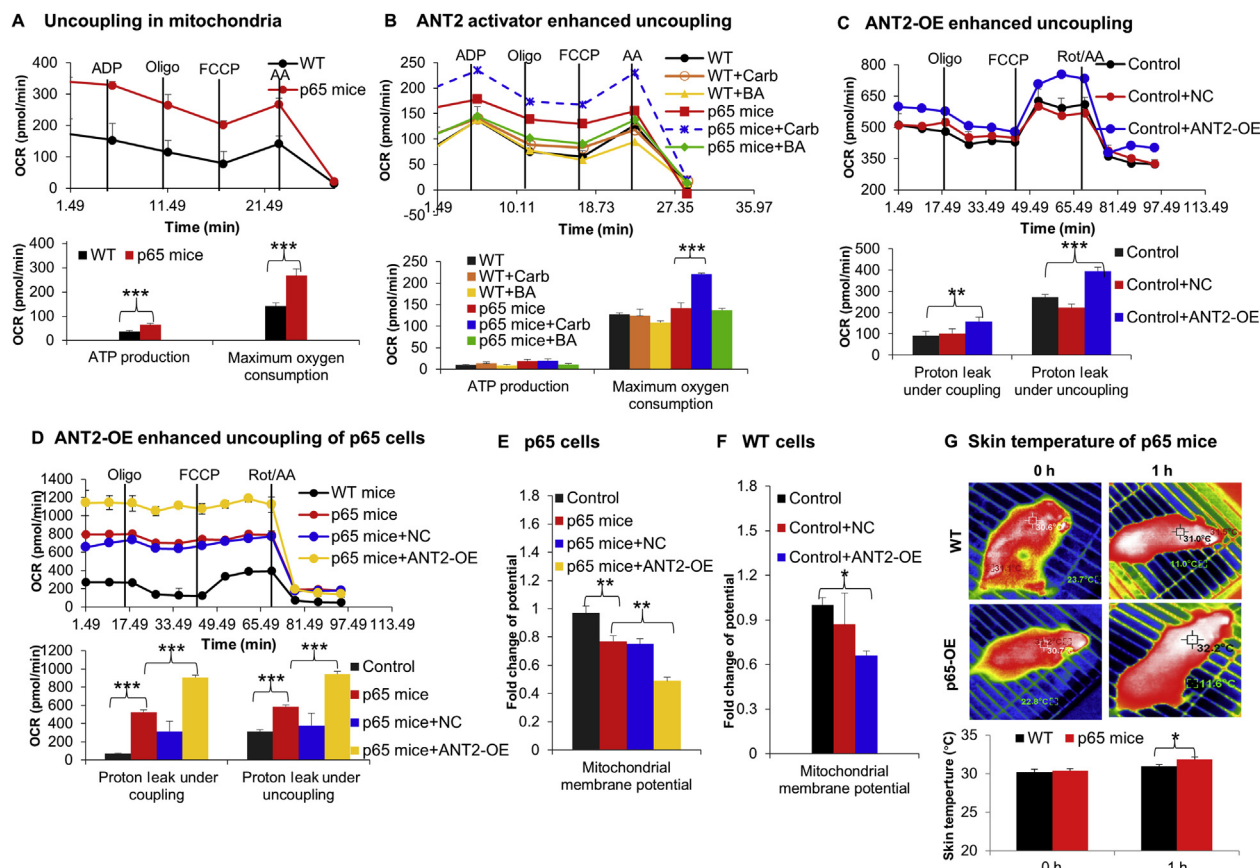
Figure 7   Uncoupling function of mitochondria under NF-κB activation. (A) Uncoupling activity of mitochondria of p65 mice. Mitochondria were isolated from fresh BAT of p65 mice and were tested for uncoupling function in MAS with 10 mmol/L succinate and 2 μmol/L rotenone. OCR was monitored in mitochondria (10 μg) in response to the chemicals and calculated for the uncoupling activity. The chemicals were ADP (4 mmol/L), oligomycin (2 μmol/L), FCCP (4 μmol/L), and antimycin (4 μmol/L) ($n = 3-4$). (B) Enhanced uncoupling function by ANT activator. ANT activity was tested in the isolated mitochondria with the agonist Carb (20 μmol/L) and inhibitor bongkrekic acid (BA, 5 μmol/L) of ANT. OCR was used in the calculation of ATP production and maximal OCR ($n = 3$). (C) *Ant2* overexpression in WT brown adipocytes. *Ant2* was overexpressed in the primary brown adipocytes (3×10^6 cells per well) of WT mice with the *Ant2* expression adenoviruses and negative control (NC) virus for 48 h. The effect of *Ant2* overexpression was tested in the cells after 48 h of infection by monitoring OCR upon injection of 1 μmol/L oligomycin, 2 μmol/L FCCP, 0.5 μmol/L rotenone plus 0.5 μmol/L antimycin (Rot/AA). Proton leak under the coupling and uncoupling conditions were calculated with OCR. (D) *Ant2* overexpression in p65-OE brown adipocytes. The overexpression effect was tested in the primary brown adipocyte of p65-OE mice. Uncoupling activity was calculated with OCR. (E) Mitochondrial membrane potential in brown adipocytes of p65-OE mice. The potential was quantified with the fluorescent dye of JC-1 by flow cytometry. (F) Mitochondrial membrane potential in brown adipocytes of WT mice. (G) Skin temperature over iBAT in the cold environment. Each experiment was repeated three times with consistent results. In the bar figure, each bar represents mean ± SD ($n = 3$). *$P < 0.05$, **$P < 0.01$, ***$P < 0.001$.

activity and reduced the mitochondrial potential, which was correlated to the increased risk of apoptosis at the same time (data not shown). In p65-KO cells, ANT2 expression was increased and the uncoupling effect was decreased, which was opposite to the activity of ANT2 in the WT cells. In the p65-OE cells, ANT2 expression was reduced, but the uncoupling activity was enhanced. The data suggest that the uncoupling activity of ANT2 was changed by the alteration of NF-κB in the transgenic mice. The ANT2 activities in the control of uncoupling may be dependent on NF-κB. The mechanism under the relationship remains unknown.

The data on mitochondrial potential suggests that an increase in mitochondrial potential is a risk of cell apoptosis. In the p65-KO cells, the rise in apoptosis was associated with the elevated mitochondrial potential. In the p65-OE cells, the decrease in mitochondrial potential was associated with reduced apoptosis. A

high mitochondrial potential is known to increase production of reactive oxygen species in the study of mitoflash under substrate overloading in mitochondria[24]. This possibility is consistent with the elevated ROS production in the condition of NF-κB inactivation in the study of JNK activation for apoptosis.

5.   Conclusions

The NF-κB activity was characterized in brown adipocytes. The data demonstrates that NF-κB activity is increased by adipocyte differentiation and cold stimulation to protect the cells from apoptosis. NF-κB is required for stabilization of mitochondrial potential and maintenance of cristae density in the control of apoptosis. The molecular mechanism is related to down-regulation of ANT2 expression in the control of apoptosis. However, it is unknown if NF-κB binds to the *ANT2* gene

promoter for a direct regulation or acts through an indirect mechanism, such as RNA modification by small RNA or methylation, etc.

Author contributions

Shiqiao Peng, Xiaoying Zhang, Lili Yu, Yanhong Xu, Yang Zhou, Shengnan Qian, Xinyu Cao, Xiaotong Ye, and Jiajun Yang conducted the experiments, analyzed the data, prepared the figures and manuscript draft. Jianping Ye and Weiping Jia had the concept, designed the study, and wrote the manuscript. All authors have read and approved the manuscript.

Declaration of competing interest

The authors declare that they have no known competing financial interests or personal relationships that could have appeared to influence the work reported in this paper.

Acknowledgments

Appendix A. Supporting information

Supporting data to this article can be found online at https://doi.org/10.1016/j.apsb.2021.10.023.

References

1. Cohen P, Kajimura S. The cellular and functional complexity of thermogenic fat. *Nat Rev Mol Cell Biol* 2021;**22**:393−409.
2. Gavalda-Navarro A, Villarroya J, Cereijo R, Giralt M, Villarroya F. The endocrine role of brown adipose tissue: an update on actors and actions. *Rev Endocr Metab Disord* 2021. Available from: https://link.springer.com/article/10.1007%2Fs11154-021-09640-6.
3. Shinoda K, Luijten IH, Hasegawa Y, Hong H, Sonne SB, Kim M, et al. Genetic and functional characterization of clonally derived adult human brown adipocytes. *Nat Med* 2015;**21**:389−94.
4. Lee YK, Chung Y, Lee JH, Chun JM, Park JH. The intricate role of p53 in adipocyte differentiation and function. *Cells* 2020;**9**:2621.
5. Kristof E, Klusoczki A, Veress R, Shaw A, Combi ZS, Varga K, et al. Interleukin-6 released from differentiating human beige adipocytes improves browning. *Exp Cell Res* 2019;**377**:47−55.
6. Li H, Dong M, Liu W, Gao C, Jia Y, Zhang X, et al. Peripheral IL-6/STAT3 signaling promotes beiging of white fat. *Biochim Biophys Acta Mol Cell Res* 2021;**1868**:119080.
7. Rajbhandari P, Thomas BJ, Feng AC, Hong C, Wang J, Vergnes L, et al. IL-10 signaling remodels adipose chromatin architecture to limit thermogenesis and energy expenditure. *Cell* 2018;**172**:218−33.
8. Rajbhandari P, Arneson D, Hart SK, Ahn IS, Diamante G, Santos LC, et al. Single cell analysis reveals immune cell−adipocyte crosstalk regulating the transcription of thermogenic adipocytes. *Elife* 2019;**8**:e49501.
9. Tang T, Zhang J, Yin J, Staszkiewicz J, Gawronska-Kozak B, Jung DY, et al. Uncoupling of inflammation and insulin resistance by NF-κB in transgenic mice through elevated energy expenditure. *J Biol Chem* 2010;**285**:4637−44.
10. Park SH, Liu Z, Sui Y, Helsley RN, Zhu B, Powell DK, et al. IKKβ is essential for adipocyte survival and adaptive adipose remodeling in obesity. *Diabetes* 2016;**65**:1616−29.
11. Jiao P, Feng B, Ma J, Nie Y, Paul E, Li Y, et al. Constitutive activation of IKKβ in adipose tissue prevents diet-induced obesity in mice. *Endocrinology* 2012;**153**:154−65.
12. Gao Z, Zhang J, Henagan TM, Lee JH, Wang H, Ye X, et al. p65 inactivation in adipocytes and macrophages attenuates adipose inflammatory response in lean but not in obese mice. *Am J Physiol Endocrinol Metab* 2015;**308**:E496−505.
13. Le J, Zhang X, Jia W, Zhang Y, Luo J, Sun Y, et al. Regulation of microbiota−GLP1 axis by sennoside A in diet-induced obese mice. *Acta Pharm Sin B* 2019;**9**:758−68.
14. Cao X, Ye X, Zhang S, Wang L, Xu Y, Peng S, et al. ADP induces blood glucose through direct and indirect mechanisms in promotion of hepatic gluconeogenesis by elevation of NADH. *Front Endocrinol* 2021;**12**:663530.
15. Gao Z, He Q, Peng B, Chiao PJ, Ye J. Regulation of nuclear translocation of HDAC3 by IκBα is required for tumor necrosis factor inhibition of peroxisome proliferator-activated receptor gamma function. *J Biol Chem* 2006;**281**:4540−7.
16. Berg AH, Lin Y, Lisanti MP, Scherer PE. Adipocyte differentiation induces dynamic changes in NF-κB expression and activity. *Am J Physiol Endocrinol Metab* 2004;**287**:E1178−88.
17. Wernstedt Asterholm I, Tao C, Morley TS, Wang QA, Delgado-Lopez F, Wang ZV, et al. Adipocyte inflammation is essential for healthy adipose tissue expansion and remodeling. *Cell Metabol* 2014;**20**:103−18.
18. Bertholet AM, Chouchani ET, Kazak L, Angelin A, Fedorenko A, Long JZ, et al. H+ transport is an integral function of the mitochondrial ADP/ATP carrier. *Nature* 2019;**571**:515−20.
19. Qin X, Xu Y, Peng S, Qian S, Zhang X, Shen S, et al. Sodium butyrate opens mitochondrial permeability transition pore (MPTP) to induce a proton leak in induction of cell apoptosis. *Biochem Biophys Res Commun* 2020;**527**:611−7.
20. Rodic N, Oka M, Hamazaki T, Murawski MR, Jorgensen M, Maatouk DM, et al. DNA methylation is required for silencing of *Ant4*, an adenine nucleotide translocase selectively expressed in mouse embryonic stem cells and germ cells. *Stem Cell* 2005;**23**:1314−23.
21. Zamzami N, Susin SA, Marchetti P, Hirsch T, Gomez-Monterrey I, Castedo M, et al. Mitochondrial control of nuclear apoptosis. *J Exp Med* 1996;**183**:1533−44.
22. Seo JB, Riopel M, Cabrales P, Huh JY, Bandyopadhyay GK, Andreyev AY, et al. Knockdown of *Ant2* reduces adipocyte hypoxia and improves insulin resistance in obesity. *Nat Metab* 2019;**1**:86−97.
23. Cho J, Zhang Y, Park SY, Joseph AM, Han C, Park HJ, et al. Mitochondrial ATP transporter depletion protects mice against liver steatosis and insulin resistance. *Nat Commun* 2017;**8**:14477.
24. Wang S, Hu M, He H. Quantitative analysis of mitoflash excited by femtosecond laser. *J Biomed Opt* 2018;**23**:1−6.